



OPEN

Direct observation of electric field-induced magnetism in a molecular magnet

M. Lewkowitz¹, J. Adams¹, N. S. Sullivan^{1✉}, Ping Wang², M. Shatruk², V. Zapf³ & Ali Sirusi Arvij⁴

We report the direct observation of an electrically-induced magnetic susceptibility in the molecular nano-magnet $[\text{Fe}_3\text{O}(\text{O}_2\text{CPh})_6(\text{py})_3]\text{ClO}_4\cdot\text{py}$, an Fe_3 trimer. This magnetoelectric effect results from the breaking of spatial inversion symmetry due to the spin configurations of the antiferromagnetic trimer. Both static and very low frequency electric fields were used. Fractional changes of the magnetic susceptibility of $11 \text{ ppb} \pm 2$ per kVm^{-1} for the temperature range $8.5 < T < 13.5 \text{ K}$ were observed for applied electric fields up to 62 kV m^{-1} . The changes in susceptibility were measured using a tunnel diode oscillator operating at liquid helium temperatures while the sample is held at a higher regulated temperature.

There is currently great interest in identifying simple molecular magnets that have quantum states that can be manipulated by external stimuli. Molecular magnets for which the magnetic and electric moments are coupled via a magnetoelectric (ME) effect^{1–7} are of particular interest both for developing an understanding of the underlying physics of the coupling mechanism, and for applications where an electric field can change the spin state. Developments in this area may open the frontier to a possible tunable quantum bit^{8,9}.

Traditionally ME effects have been studied in inorganic oxides and/or materials with long-range magnetic and/or electric order. In paramagnetic non-interacting molecules, a different mechanism for a ME coupling exists, where the local spin configuration of each molecule can break inversion symmetry and create an electric dipole. For example, Dzyaloshinski-Moriya (DM) interactions^{10,11} can produce magnetic spin states in triangles that are non-centro-symmetric and polar. Plokhov et al.¹² have shown that chirality can be induced in rare-earth spin clusters to result, in some cases, in electric dipoles.

We have studied frustrated spin triangles with anti-ferromagnetic couplings that possess spin chirality as a result of the combined effect of frustrated exchange interactions and a Dzyaloshinski-Moriya interaction. Trif et al.² and Bulaevskii et al.¹³ have proposed that the chirality eigen-value could be used as a qubit. These systems have a spin chirality that can be probed as the magnetic state is varied over a wide temperature range. Sowrey et al.¹⁴ have pointed out that the trinuclear oxo-centered carboxylate bridged complexes of the general formula $[\text{M}_3^{\text{III}}\text{O}(\text{O}_2\text{CR})_6\text{L}_3]^+$, and in particular $[\text{Fe}_3\text{O}(\text{O}_2\text{CPh})_6(\text{py})_3]\text{ClO}_4\cdot\text{py}$ have the desirable symmetry, with half of the Fe^{3+} ions forming an isosceles triangle, and the other half of the ions forming a scalene triangle as shown in Fig. 1. The molecules can be static or undergoing dynamic pseudo-rotations.

Indirect observation of an ME effect in the Fe_3 trimer, $[\text{Fe}_3\text{O}(\text{O}_2\text{CPh})_6(\text{py})_3]\text{ClO}_4\cdot\text{py}$, has been reported by Boudalis et al.¹⁵. The amplitudes of the electron paramagnetic resonance (EPR) absorption lineshapes were modified by a few percent for static electric fields up to 10^9 V m^{-1} but no displacements of the EPR line position were reported. George et al.¹⁶ have reported a ME effect for the antiferromagnetic wheel Cr_7Mn in studies of the electron spin resonance (ESR) echo. In this paper we report direct observation of the ME coupling for a small electric field in crystalline samples of the aforementioned Fe_3 cluster. There have been a few observations of ME effects already reported for molecular magnets^{15,16}, but we report here what we believe is the first direct low frequency measurement.

¹Department of Physics, University of Florida, Florida 32611, USA. ²Department of Chemistry and Biochemistry, Florida State University, Florida 32306, USA. ³Los Alamos National Laboratory, Los Alamos, NM 87545, USA. ⁴School of Science, Mathematics and Engineering, San Juan College, Farmington, NM 87402, USA. ✉email: sullivan@phys.ufl.edu

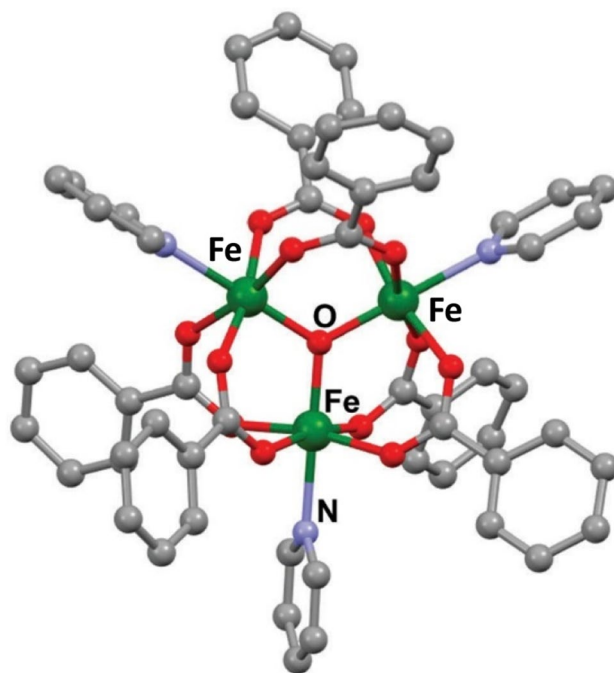


Figure 1. (Color online) Structure of the Fe₃ carboxylate trimer as reported by Sowrey *et al.*¹⁴. Created from the Cambridge Crystallographic Data Base (entry code QOPLUC).

Experimental methods

The sample of Fe₃ consisted of one mm-sized crystal and two smaller crystals (< 0.5 mm) glued together with Apiezon N-grease¹⁷ with the c-axis aligned parallel to the RF magnetic field of the oscillator. Two electrodes inside the RF coil provided an electric field perpendicular to the c-axis. The filling factor for the samples was of the order of 2%. The N-grease also served to thermalize the crystals to the regulated thermal block. N-grease by itself does not have a high thermal conductivity (typically 100 mW/Km at 4 K¹⁸, but it readily fills the micropores of adjoining surfaces and is thus excellent for thermal contact to the surface of a crystal at low temperatures. Furthermore, the N-grease does not lower the electronic quality factor (Q) of the resonant circuit.

The ME effect was observed using an ultra-high sensitivity tunnel diode oscillator (TDO)¹⁹ operating at low temperatures to measure changes in the magnetic susceptibility of the order of parts per billion (ppb). A schematic representation of the oscillator system is shown in Fig. 2. The tunnel diode was maintained continuously at liquid helium temperatures for high sensitivity and high stability while the sample coil was thermally isolated from the TDO circuit and independently thermalized to a reference block whose temperature could be regulated between 3 and 120 K very precisely with a feedback loop. The sample was located inside a solenoidal radio frequency (RF) coil that oscillated at 15 MHz. The frequency was read by a precision frequency counter and digitized for sample averaging as the electric field was slowly modulated with a triangular wave shape having a period of 120 s. Data was also taken with a fixed electric field of 62 kV m⁻¹ as the temperature was swept slowly at a rate of 2.5 K hr⁻¹ from 8.5 to 13.5 K. This temperature range was selected because the susceptibility studies of Georgopoulou *et al.* showed that in this temperature range the susceptibility is most affected by the antisymmetric exchange.

The change in susceptibility is determined from the fractional change in the oscillator frequency as a function of the temperature and field dependent magnetic susceptibility, $\chi(E, T)$, from

$$\frac{\delta f}{f} = -0.5\eta\chi'(E, T) + O(Q^{-2}\chi'') \quad (1)$$

where I_0 is the coil filling factor, Q the coil quality factor, and χ' and χ'' are the real and imaginary components of the magnetic susceptibility. The term in Q^{-2} can be neglected as Q is of the order of 10³ at low temperatures.

Synthesis of [Fe₃O(O₂CPh)₆(py)₃]ClO₄·py (Fe₃). Iron(III) perchlorate hydrate, benzoic acid, and pyridine were obtained from VWR and used as received. (Caution: Complexes between metal ions and organic ligands with perchlorate anions are potentially explosive. The compounds should be prepared in small amounts and handled with great care!) The synthesis of Fe₃ was carried out according to the published procedure¹⁴.

Briefly, 1.44 g (≈ 3.1 mmol) of Fe(ClO₄)₃·xH₂O (x ≈ 6) was added with stirring to a solution of benzoic acid (1.22 g, 10.0 mmol) in 10 mL of pyridine. The resulting suspension was refluxed for 1.5 h and then allowed to cool to room temperature. After filtration, the filtrate was left to evaporate slowly on a warm heating plate (≈ 35°C), to afford X-ray quality crystals of Fe₃. The reported unit cell was confirmed by single-crystal X-ray diffraction

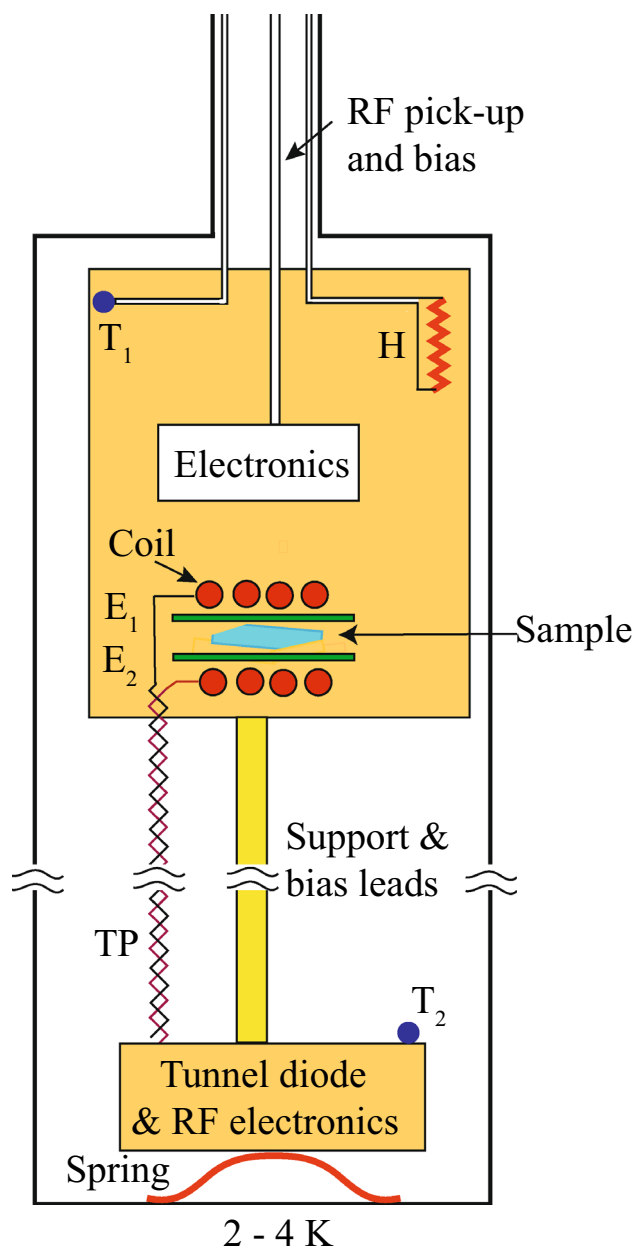


Figure 2. (Color online) Schematic representation of experimental apparatus (not to scale). The tunnel diode and associated bias circuit are located in the bottom block that is pressed against a cold plate at liquid helium temperatures. The support (yellow) maintains the pressure for the thermal contact. The resonant coil is located on a separate thermal block whose temperature is regulated by a feedback circuit feeding a heater H. The temperatures are measured with calibrated Cernox resistors^{18,19} T₁ and T₂. The separation between the sample block and the tunnel diode allows one to regulate the sample temperatures from 3.0 to 120 K. The twisted pair TP connects the tunnel diode to the resonant coil. Two electrodes (green) provide the electric field.

as reported in the Cambridge Crystallographic Data base (code [QOPLUC](#)). The compound forms in the centrosymmetric P6₃/m space group and consists of trimers of Fe spins that are isolated from each as shown in Fig. 1.

Results and discussion

The ultimate sensitivity of the TDO is determined by the shot noise of the device and the thermal stability of the diode. Robinson²³ has shown that the shot noise in the current is given by

$$I_n = \sqrt{4eI_0B(1 + f_0/f)} \quad (2)$$

where I_0 is the operating current, B is the post detection bandwidth and the corner frequency

$$f_o \approx 10^3 \text{ Hz.}$$

The sensitivity to changes in diode conductance G is therefore

$$\frac{\delta G}{G} = \sqrt{4Fk_B T B Q / P_0} \quad (3)$$

for a power level P_0 . With a noise factor $F \approx 10$, this leads to a sensitivity of the order of 10^{-9} for an integration time $B^{-1} \approx 10$ s., which might be improved by averaging over a longer time.

The thermal variations were more troublesome (due to long internal time constants for the diode) and most of the fluctuations in the frequency of the oscillator with an empty cell were due to variations in temperature rather than shot noise. We therefore recorded data with the temperature for a very slow sweep with $\Delta T \approx 0.1 \text{ K} \cdot \text{hr}^{-1}$ (to keep the feedback circuit active) and modulated the applied electric field using a triangular amplitude as a function of time. The data were analyzed assuming a form

$$f_k = g(T_k, E_k) + \xi_k \quad (4)$$

for each data point f_k where $g(T_k, E_k)$ is a model for the frequency response for an electric field E_k and a temperature T_k . \tilde{g} is a fit to the data after averaging and ξ_k is a random noise function.

The average $\tilde{g}_k = C_{0k} + C_{T_k} T + C_{E_k} E$ was found by minimizing $\sum_{l=k-n}^{k+n} [f_l - \tilde{g}_i(T_l, E_l)]^2$ for n sweeps. Assuming $\tilde{g}(T_l, E_l) = g(T_l, E_l) + \mathcal{O}(\frac{1}{\sqrt{n}})$ we have (using MKS units)

$$\tilde{g}_k(T_k, E_k) - \tilde{g}_k(T_k, 0) = -\frac{1}{2} \eta \left(E \frac{\partial \chi'}{\partial E} \right)_k \quad (5)$$

Figure 3 clearly shows that the frequency response resulting from the susceptibility change is synchronous with the time dependence of the electric field. The amplitude of the observed ME effect

is indeed small at $16 \text{ ppb} \pm 3$ per kV m^{-1} . This value is within the range estimated theoretically by Yu et al.²⁴ who predicted a quadratic effect but for a different material, namely Mn_4Te_4 which has tetrahedral spin frustration, in contrast to the Fe_3 - trimer which has triangular frustration and thus could have a very different ME effect. The experiment was repeated for an empty cell but containing N-grease and no ME effect was observed.

The results presented here do not have the resolution to test that prediction. Nevertheless, the results can be compared with the observation of Boudalis *et al.*¹⁵ who found approximately a 1% effect for 10^9 V m^{-1} , or 10 ppb per kV m^{-1} which would be consistent with the results reported here for a linear effect. In order to obtain a better test the linear electric field dependence we would need to be able to apply an appreciably higher electric field, or modify the detector to obtain much higher sensitivity. Increasing the electric field to increase the magnitude of the effect is precluded because of voltage breakdown at small interfaces in the wiring at low temperatures, but improved sensitivity could be obtained by designing an ultra-high frequency (UHF) cavity resonator and that is being actively pursued. Conducting the experiments at much lower temperatures would run into problems with the long relaxation times at those temperatures.

The data for a fixed electric field is shown in Fig. 4. While there is a detectable effect shown by the red arrow, the variation in noise amplitude from one temperature to another at a later time was quite large. We have therefore averaged the electric field induced changes over several temperature sweeps, and assuming the paramagnetic temperature dependence of Ref. 19, we find the average magnitude of the ME effect over this full temperature range to be $11 \text{ ppb} \pm 2$ per kV m^{-1} . This value is consistent with the results of Boudalis et al.¹⁵.

Thus, we have observed electric field-induced changes in the magnetic susceptibility in Fe_3 , which is a direct observation of ME coupling. We note that the Fe_3 compound forms in a centrosymmetric space group $P6_3/m^{14}$, whereas a ME coupling requires broken centrosymmetry. Thus any observed ME coupling indicates that centrosymmetry has become broken by the magnetic configuration of the Fe spins. Such spatial inversion symmetry breaking is predicted to occur in antiferromagnetic triangles like Fe_3 via magnetic frustration and/or DM interactions^{2,4,13,24}, both of which are present in this material. In general, the microscopic mechanisms by

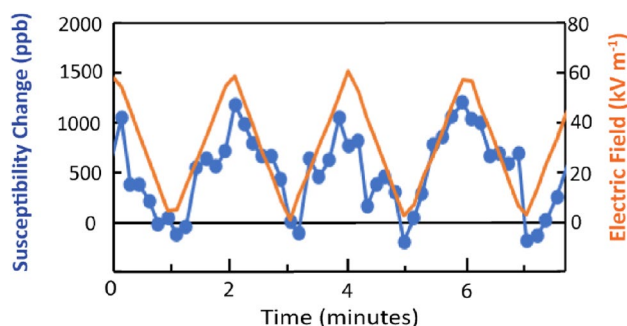


Figure 3. (Color online) Observed variation of magnetoelectric effect of the Fe_3 trimer with a slow modulation of the applied electric field with peak field at 62 kV m^{-1} . The electric field was aligned perpendicular to the RF magnetic field which was parallel to the c-axis of the crystal. The blue circles are the data points for the changes in magnetic susceptibility and the orange trace is the electric field.

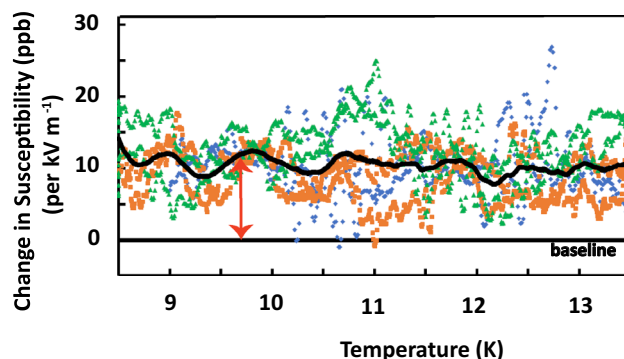


Figure 4. (Color online) Observed shift of magnetic susceptibility of the Fe_3 trimer for a fixed applied electric field for several temperature sweeps. The blue, green and orange data points are the direct observations of the changes for four different sweeps with no averaging, and the solid black line is a filtered overall average as described in the text.

which magnetic configurations can induce electric dipoles in all materials involves (1) magnetostriction, e.g. distortion of the location of the charged ions in the lattice and/or (2) rearrangements of the electronic orbitals. These changes in the lattice and orbitals are driven by a need to minimize the magnetic energy at the expense of lattice distortion energy by modifying interactions such as magnetic exchange, single-ion anisotropy, or DM interactions.

Conclusion

Studies of the influence of an applied electric field on the magnetic susceptibility of an Fe_3 trimer, $[\text{Fe}_3\text{O}(\text{O}_2\text{CPh})_6(\text{py})_3]\text{ClO}_4\cdot\text{py}$, using a stabilized cryogenic tunnel diode oscillator, have revealed the existence of a small electrically-induced change in the magnetic susceptibility, of $11 \text{ ppb} \pm 2 \text{ per kV m}^{-1}$ for $8.5 < T < 13.5 \text{ K}$. The overall magnitude is in the range of the theoretical results by Yu et al.²² and is consistent with the change in ESR amplitude reported by Boudalis et al.¹⁵. It will be important to extend these studies to higher sensitivities, for example, by increasing the frequency of the oscillator to the 200–250 MHz range. This extension will also provide information about dynamics of the magnetic spin system and its dependence on the electric field.

Data availability

The datasets generated and/or analysed during the current study are available in the Cambridge Crystallographic Data Centre (CCDC) repository, and can be retrieved from the CCDC by referring to the entry code [QOPLUC](#).

Received: 14 November 2022; Accepted: 10 February 2023

Published online: 16 February 2023

References

- Kane, B. E. A silicon-based nuclear spin quantum computer. *Nature* **393**(133), 137 (1998).
- Trif, M., Troiani, F., Stepanenko, D. & Loss, D. Spin-electric coupling in molecular magnets. *Phys. Rev. Lett.* **101**, 217201 (2008).
- Trif, M., Troiani, F., Stepanenko, D. & Loss, D. Spin electric effects in molecular antiferromagnets. *Phys. Rev. B* **82**, 045429 (2010).
- Islam, M. F., Nossa, J. F., Canali, C. M. & Pederson, M. First-principles study of spin-electric coupling in a Cu_3 single molecular magnet. *Phys. Rev. B* **82**, 155446 (2010).
- Naka, M. & Ishihara, S. Magnetolectric effect in organic molecular solids. *Sci. Rep.* **6**, 20781 (2016).
- Fittipaldi, M. et al. Electric field modulation of magnetic exchange in molecular helices. *Nat. Mater.* **18**, 329 (2019).
- Liu, J. et al. Electric field control of spins in molecular magnets. *Phys. Rev. Lett.* **122**, 037202 (2019).
- Bogani, L. & Wernsdorfer, W. Molecular spintronics using single-molecule magnets. *Nat. Mater.* **7**, 179 (2008).
- Khomskii, D. I. Spin chirality and nontrivial charge dynamics in frustrated Mott insulators: spontaneous currents and charge redistribution. *J. Phys. Condens. Matter* **22**, 164209 (2010).
- Dzyaloshinsky, I. A thermodynamic theory of “weak” ferromagnetism of antiferromagnetics. *Journ. Phys. and Chem. Solids* **4**, 241 (1958).
- Moriya, T. Anisotropic superexchange interaction and weak ferromagnetism. *Phys. Rev.* **120**, 91 (1960).
- Plokhov, D. I., Zvezdin, A. K. & Popov, A. I. Macroscopic quantum dynamics of toroidal moment in Ising-type rare-earth clusters. *Phys. Rev. B* **83**, 184415 (2011).
- Bulaevskii, L. N., Batista, C. D., Mostovoy, M. V. & Khomskii, D. I. Electronic orbital currents and polarization in Mott insulators. *Phys. Rev. B* **78**, 024402 (2008).
- Sowrey, F. E. et al. Spin frustration and concealed asymmetry, structure and magnetic spectrum of $[\text{Fe}_3\text{O}(\text{O}_2\text{CPh})_6(\text{py})_3]\text{ClO}_4\cdot\text{py}$. *J. Chem. Soc. Dalton Trans.* **6**, 862 (2001).
- Boudalis, K., Robert, J. & Turek, P. First demonstration of magnetolectric coupling in a polynuclear molecular nanomagnet: Single-crystal EPR studies of $[\text{Fe}_3\text{O}(\text{O}_2\text{CPh})_6(\text{py})_3]\text{ClO}_4(\text{py})$ under static electric fields. *Chem. Eur. J.* **24**, 14896. <https://doi.org/10.1002/chem.201803038> (2018).
- George, R. E., Edwards, J. P. & Ardavan, A. Coherent spin control by electrical manipulation of the magnetic anisotropy. *Phys. Rev. Lett.* **110**, 027601 (2013).
- Apiezon type N-grease, M & I Materials Ltd, Manchester.
- Pobell, F. *Magnetics and Methods at Low Temperatures* 3rd edn. (Springer Publishing, 2006).
- Georgopoulou, N., Margiolaki, I., Psycharis, V. & Boudalis, A. K. *Inorg Chem* **56**(2), 762–772 (2017).

20. Gati, E. *et al.* Use of Cernox thermometers in AC specific heat measurements under pressure. *Rev. Sci. Instrum.* **90**, 023911. <https://doi.org/10.1063/1.5084730> (2019).
21. Courts, S. S. & Swinehart, P. R. Review of Cernox™ (zirconium oxy-nitride) thin-film resistance temperature sensors. *AIP Conf. Proc.* **684**, 393. <https://doi.org/10.1063/1.1627157> (2003).
22. Sirusi, J. Adams, M. Lewkowitz, R. Sun, and N. S. Sullivan, *A tunnel diode oscillator for high sensitivity broad temperature range susceptibility measurements* (2021), [arXiv:2109.11030](https://arxiv.org/abs/2109.11030) [physics.ins-det].
23. Robinson, F. N. H. A magnetic resonance spectrometer for 100–1200 MHz. *Journ. of Physics E: Sci. Instrum.* **10**, 254 (1977).
24. Yu, J.-X., Chen, J., Sullivan, N. & Cheng, H.-P. Dzyaloshinskii-Moriya interaction induced magnetoelectric coupling in a tetrahedral molecular spin-frustrated system. *Phys. Rev. B* **106**, 054412 (2022).

Acknowledgements

We thank the University of Florida Physics Department machine shop for the fabrication of parts of the experimental cell. This work was supported as part of the University of Florida's Center for Molecular Magnetic Quantum Materials, an Energy Frontier Research Center funded by the U.S. Department of Energy, Office of Science, Basic Energy Sciences Program under Award # DE-SC0019330. Part of VSZ's effort was supported by the National High Magnetic Field Laboratory, funded by the US National Science Foundation, the Department of Energy and the State of Florida through the NSF Cooperative Grant No. DMR-1644779.

Author contributions

M.L., J.A. and A.S.A. designed, constructed and operated the apparatus and carried out the primary data analysis. M.S. and P.W. prepared the sample and advised on sample installation and sample properties. N.S. proposed and oversaw the experiment, and crafted the manuscript. V.Z., (group leader of M2QM research on magnetoelectric effects) provided information on underlying physics of magnetoelectric phenomena and advised on experimental procedures. All authors contributed to the writing of the manuscript and are members of the M2QM Center for Research on quantum magnetism.

Competing interests

The authors declare no competing interests.

Additional information

Correspondence and requests for materials should be addressed to N.S.S.

Reprints and permissions information is available at www.nature.com/reprints.

Publisher's note Springer Nature remains neutral with regard to jurisdictional claims in published maps and institutional affiliations.



Open Access This article is licensed under a Creative Commons Attribution 4.0 International License, which permits use, sharing, adaptation, distribution and reproduction in any medium or format, as long as you give appropriate credit to the original author(s) and the source, provide a link to the Creative Commons licence, and indicate if changes were made. The images or other third party material in this article are included in the article's Creative Commons licence, unless indicated otherwise in a credit line to the material. If material is not included in the article's Creative Commons licence and your intended use is not permitted by statutory regulation or exceeds the permitted use, you will need to obtain permission directly from the copyright holder. To view a copy of this licence, visit <http://creativecommons.org/licenses/by/4.0/>.

© The Author(s) 2023